CALCULATION OF FLOW OVER MULTIELEMENT AIRFOILS AT HIGH LIFT

Tuncer Cebeci
Center for Aerodynamics Research
California State University, Long Beach, California

K. C. Chang, R. W. Clark and N. D. Halsey
Aerodynamics Research and Technology
Douglas Aircraft Company, Long Beach, California

Abstract

An interactive boundary-layer procedure has been used to calculate the flow around three two-element airfoil arrangements. The procedure is known to be accurate, is seen as the foundation of a generally applicable calculation method and is used here in comparatively simple form. The calculated results are in close agreement with measurements for angles of attack up to around 10 degrees, with flap-deflection angles of up to 20 degrees. The range of accuracy of the predictions can be extended by incorporation of the wake and this will be required to deal with high angles of attack, high flap deflection angles and airfoil elements with smaller slot gaps than those considered here.

1.0 Introduction

As high-lift devices increased in complexity, there was a corresponding increase in the wind-tunnel time dedicated to their development. Attempts to reduce the wind-tunnel time by developing calculation methods were a natural consequence. The hope was that unpromising configurations could be eliminated quickly and the wind tunnel used for final refinement only. Initial attempts were confined mostly to inviscid flow methods and advances were limited by experimental information which usually comprised only force data and pressure distributions. This situation prompted more detailed experimental investigations and it was discovered, for example, that with a simple slotted flap in optimum position, maximum performance often involved regions of separated flow which extended into the wake. The immediate consequence of the presence of separated flow is that the inviscid-viscous interaction can no longer be treated as a small perturbation about inviscid flow effect, but rather as a strong interaction which requires an inverse boundary-layer approach. In addition, there is a clear need to represent transition, and its relationship to flow separation.

The emphasis of the present work on two-dimensional flows is justified by the general view that two-dimensional information is applicable to the three-dimensional flow over wings for high aspect-ratio configurations. Thus, although well-founded corrections for finite span, sweep and taper are not available, two-dimensional testing is often preferred.

Early prognostications for interactive calculations were optimistic and, for example, the method developed at NASA[1] and making use of integral equations for the viscous flow, was clearly inappropriate where separation occurred and could not represent maximum lift. The introduction of finite-difference methods to solve boundary-layer equations in differential form led to greater flexibility in that merging boundary layers could be represented even where small regions of flow separation occurred and a range of turbulence-models could be incorporated readily. It is evident, for example in reference 2, that useful results can be obtained for two-element airfoils but, in spite of an attached flow and selective use of turbulence models, improvements were called for. An alternative approach based on representing the separated flow by distributed sources led to its use in the design process[3] but the review of reference 4 makes it very clear that the value of the computational methods of this period was limited.

Recent interactive procedures, for example those of[5-9], involve more accurate and flexible solution methods for the inviscid and boundary-layer flows so that complex geometries can be considered and the solution domain can encompass regions of separated flow and the downstream wake. To advance the abilities of calculation methods beyond that described in reference 4, it is necessary to combine the most powerful components and to develop the resulting method in conjunction with available experimental data. This plan of attack is carried forward in this paper by using the interactive procedure[10], which involves the conformal-mapping approach to the solution of the inviscid-flow equations[11] and the inverse finite-difference solution of the boundary-layer equations[12], to calculate the two-element airfoil flows investigated in references 13,14,15. In this early step in the development plan, the wakes from the two airfoil elements are not included in the calculations and incompressible equations are solved. These restrictions can be removed and will become important at high angles of attack with small gaps between airfoil elements and in the presence of flap wells: in the cases considered here, however, they are of less importance, as will be shown. As demonstrated many years ago[16], the wake from the first element frequently does not interact with the upper-surface boundary layer of the second element and, in maximum lift, upper surface separation can reduce the influence of the wake from the second element. Also, compressibility is unlikely to be of importance in the present flows though, in some cases with high velocity peaks at the leading edge, it will be necessary to involve a compressible form of the conformal-mapping method, such as that described in reference 17.

The following section provides a description of the interactive procedure used to obtain the results of Section 3. The paper ends with a summary of the main conclusions and a statement of the further steps which will be taken toward the provision of a general method for the calculation of the flow around high-lift devices.

2.0 The Interactive Boundary-Layer Method

The results of the following section correspond to two-element airfoils and were obtained by interaction of solutions of the inviscid- and viscous-flow equations. The inviscid flow around the two elements was obtained by solving the inviscid-flow equations with the conformal-mapping procedure[11]. The resulting surface-pressure distribution was used as the external boundary condition in the solution of the boundary-layer equations for each surface of the two elements which, in turn, determines a surface blowing distribution to simulate the displacement-thickness effect. The inviscid-flow equations are then re-solved with a distribution of normal velocity on the surface obtained from

$$V_n = \frac{d}{ds}(u_e \delta^*) \tag{1}$$

The new pressure distribution is used again in the boundary-layer method and the procedure is repeated until convergence.

Where the calculation encounters separation, the inverse solution of the boundary-layer equations, together with the FLARE assumption[18] allowed results to be obtained. In all cases, the viscous-flow calculation was terminated at the trailing edge.

The following section provides a brief description of the formulation of the boundary-layer scheme and its solution procedure. The inviscid method is described in detail in reference 11 and is not repeated here. Similarly, the turbulence model is based on that of Cebeci and Smith and a detailed description of the form used here is available in reference 10.

2.1 Formulation of the Interactive Scheme

For two-dimensional external steady incompressible flows, the boundary-layer equations are well known and, with the concept of eddy viscosity ν_t and with b denoting $1 + \nu_t/\nu$, can be written as

$$\frac{\partial u}{\partial x} + \frac{\partial v}{\partial y} = 0 \tag{2}$$

$$u\frac{\partial u}{\partial x} + v\frac{\partial u}{\partial y} = u_e\frac{du_e}{dx} + \nu\frac{\partial}{\partial y}\left(b\frac{\partial u}{\partial y}\right) \tag{3}$$

The boundary conditions, in the absence of mass transfer, are

$$y = 0 \qquad u = v = 0 \tag{4a}$$

$$y \to \infty \qquad u \to u_e(x) \tag{4b}$$

In Eqs. (3) and (4b) the external velocity distribution $u_e(x)$ is obtained either from experiment or from inviscid flow theory. In the latter case, it is often necessary to consider the effect of the displacement thickness on the calculated velocity distribution and this can be done in several ways. Here, as in reference 10, we write the edge boundary condition, with $u_e^o(x)$ denoting the inviscid velocity distribution and $\delta u_e(x)$ the perturbation velocity due to viscous effects, as

$$u_e(x) = u_e^o(x) + \delta u_e(x) \tag{5}$$

and assume that the interaction region is limited to a finite range $x_a \le x \le x_b$. The perturbation velocity, $\delta u_e(x)$, is determined from the Hilbert integral

$$\delta u_e(x) = \frac{1}{\pi}\int_{x_a}^{x_b} \frac{\frac{d}{d\sigma}(u_e\delta^*)}{x - \sigma}\, d\sigma \tag{6}$$

where $d(u_e\delta^*)/d\sigma$ is the blowing velocity. Following reference 10, we write Eqs. (5) and (6) as

$$u_e(x) = u_e^o(x) + \sum_{j=1}^{n} c_{ij}(u_e\delta^*)_j \tag{7a}$$

Here c_{ij} denotes the interaction-coefficient matrix, which is obtained from a discrete approximation to the Hilbert integral in Eq. (6). In this form, Eq. (7a) provides an outer boundary condition for the viscous-flow calculation which represents the viscous/inviscid interaction. It can be generalized to the form

$$u_e(x) = u_e^K(x) + \sum_{j=1}^{n} c_{ij}[(u_e\delta^*)_j - (u_e\delta^*)_j^K] \tag{7b}$$

where $u_e^K(x)$ corresponds to the inviscid velocity distribution which contains the displacement thickness effect, $(\delta^*)^K$, computed from a previous sweep.

As discussed in reference 19, it is more convenient to solve Eqs. (2) and (3) when they are expressed in transformed variables. In the early stages of the boundary-layer development, the Falkner-Skan transformation is used for this purpose. This transformation provides the generation of initial conditions at the stagnation point of the airfoil and allows the calculations to be performed economically and accurately around the leading edge, where the governing equations are being solved for the prescribed external velocity distribution. For interactive boundary-layer calculations, where $u_e(x)$ is not known, a constant reference velocity u_o is used in the transformation

$$Y = \sqrt{u_o/\nu x}\, y, \qquad \psi = \sqrt{u_o \nu x}\, F(x,Y) \tag{8}$$

and in terms of these new variables, Eqs. (2) and (3) and their boundary conditions are written in the form:

$$(bF'')' + \frac{1}{2}FF'' + xw\frac{dw}{dx} = x\left(F'\frac{\partial F'}{\partial x} - F''\frac{\partial F}{\partial x}\right) \tag{9}$$

$$Y = 0, \qquad F = F' = 0 \tag{10a}$$

$$Y = Y_e, \qquad F' = w, \qquad w - \dot{c}_{ij}(Y_e w - F) = g_i \tag{10b}$$

Here primes denote differentiation with respect to Y and

$$\dot{c}_{ij} = c_{ij}\sqrt{\nu x/u_o}, \qquad w = \frac{u_e}{u_o} \tag{11}$$

The parameter g_i, which results from the discrete approximation to Eq. (7) is given by

$$g_i = \bar{u}_e^K + \sum_{j=1}^{i-1} c_{ij}(D_j - D_j^K) - c_{ii}D_i^K \tag{12}$$

where

$$D = \sqrt{\nu x/u_o}\,(Y_e w - F_e)$$

2.2 Solution Procedure

The numerical solution of the system of equations given in the previous section is obtained with Keller's box method for the standard and interactive methods. This is an efficient, second-order finite-difference method extensively used by Cebeci and his associates for a wide range of flows, as discussed in Bradshaw et al.[19]. The description of the standard method is given in that reference as well as in Cebeci and Bradshaw[20]. The general features of the inverse method which makes use of the Mechul-function formulation are also described for wall boundary layers in Bradshaw et al.[19]. As in previous studies the FLARE approximation in which the convective term $\partial F'/\partial x$ is set equal to zero in the recirculating region is employed, and no attempt was made to improve the accuracy of the solutions resulting from this approximation.

As in the solution of wall boundary-layer flows by Keller's method, we write Eq. (9) as a first-order system. For this purpose we let

$$F' = u \tag{13a}$$

$$u' = v \tag{13b}$$

and write Eq. (9) as

$$(bv)' + \frac{1}{2} Fv + xw \frac{dw}{dx} = x\left(u \frac{\partial u}{\partial x} - v \frac{\partial F}{\partial x}\right) \tag{13c}$$

Since w is a function of x, only, we write

$$w' = 0 \tag{13d}$$

The boundary conditions for the system given by Eqs. (13) now can be written as

$$Y = 0, \qquad F = 0, \qquad u = 0 \tag{14a}$$

$$Y = Y_e, \qquad u = w, \qquad w - c_{ij}(Y_e w - F) = g_i \tag{14b}$$

After the finite-difference approximations to Eqs. (13) and (14) are written, the resulting nonlinear algebraic system is linearized by Newton's method and then solved by the block-elimination method. For further details, see references 19 and 20.

3.0 Results

Calculations were performed for the flow configurations described in references 13,14 and 5. The calculations required, for each configuration, a few seconds of CRAY time and were performed without computational difficulties.

The two-element arrangement of Olsen and Orloff[13] involved a NACA 4412 airfoil with a chord length of 0.9m upstream of a flap which had the section of a NACA 4415 airfoil and a chord of 0.36m. The freestream Mach number was 0.06 and the experiment was conducted in the 7 x 10 ft wind tunnel at NASA Ames Research Center. One configuration was investigated and is shown in Figure 1 together with the measured and calculated surface-pressure distributions for this case, which exhibit similar trends. It is likely that the quantitative difference is, in part, due to wind-tunnel blockage but the magnitude of the difference in the two results is impossible to explain with certainty. This exemplifies one of the problems associated with the development of calculation methods and with the interpretation of measurements.

The second case involves a NASA supercritical airfoil, 24 in. in length, with a 7 in. flap at a deflection angle of 20 degrees. The experiments were carried out in the 36 x 96 in. wind tunnel of the Boeing Research Laboratories at a Mach number of 0.2 and have been documented by Omar, Ziertan and Mahal[14] and by Omar, Zierten, Hahn, Szpiro and Mahal[21]. Figure 2 shows the configuration at zero angle of attack and the surface-pressure distributions: the agreement between calculation and experiment is within the measurement uncertainty. Figure 3 shows similar results at 8.93 degrees angle of attack and differences similar to those of Figure 1 occur on the upper surface of the airfoil and flap. They do not appear to be connected with transition which occurred naturally in the experiment and was computed by Michel's formula[22] in the calculation. It is possible that a transport model of turbulence would reduce the difference but unlikely that the improvement would be significant. The influence of angle of attack of the airfoil system is shown in Figs. 4 and 5, which present the lift coefficient and displacement-thickness variations. The need for the interactive procedure, rather than the inviscid calculation alone, is made clear by Fig. 4, which also reveals very good agreement over a wide range of angles. It is interesting that upper surface separation appears to exist only on the flap and probably explains the ability to make acceptable calculations without consideration of the wakes of the main airfoil: of course, where the gap between elements is small, the wake effects will have to be properly represented.

The third case corresponds to that investigated by van den Berg[15] and discussed in subsequent papers by van den Berg and Oskam[2] and Oskam, Laan and Volken[23]. It comprised a supercritical main airfoil (NLR 7301) with a flap, of 32% of the main chord, at a deflection angle of 20 degrees. This flap angle was close to the highest value which could be used without onset of flow separation. The arrangement is shown on Fig. 6 together with the surface-pressure distributions an angle of attack of 6 degrees; as with the former case, at zero angle of attack, the calculated results agree with the measurements within measurement uncertainty. At 13.1 degrees, Fig. 7, the pressure distribution on the main airfoil is again well represented, but that on the upper surface of the flap is overpredicted probably due to interaction between the upper-surface boundary layer and the wake of the main airfoil. As can be seen from the distributions of skin-friction coefficient, Fig. 8, the boundary layer on the upper surface is approaching separation but has not reached it so that the wake is likely to be highly curved. The results of Fig. 8 confirm that the properties of the viscous layer are well represented by the algebraic eddy-viscosity hypothesis described in reference 10 and recover rapidly from the simple approach used, embodied in the correlation equation, to represent transitional region.

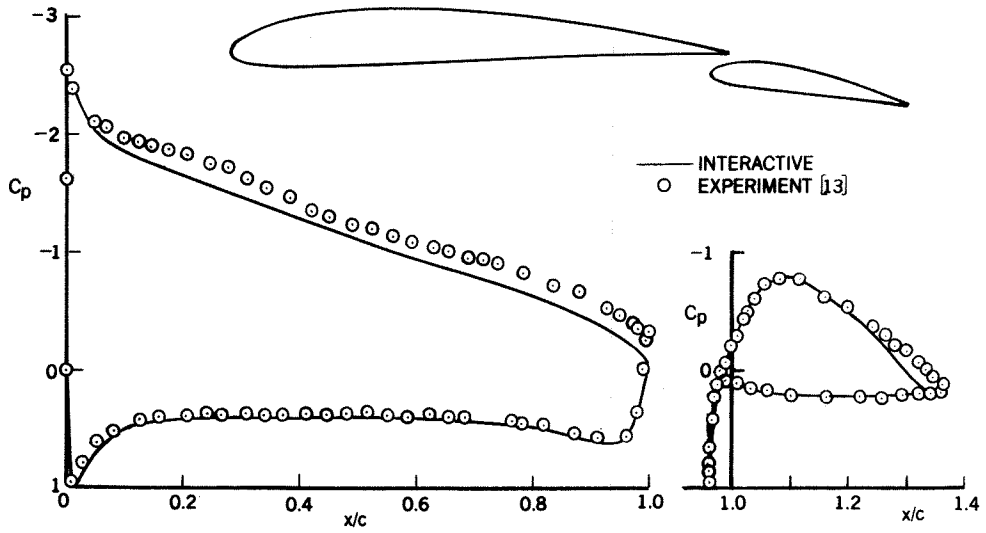

Figure 1. Comparison of calculated and measured pressure distribution for the data of Olsen and Orloff[13].

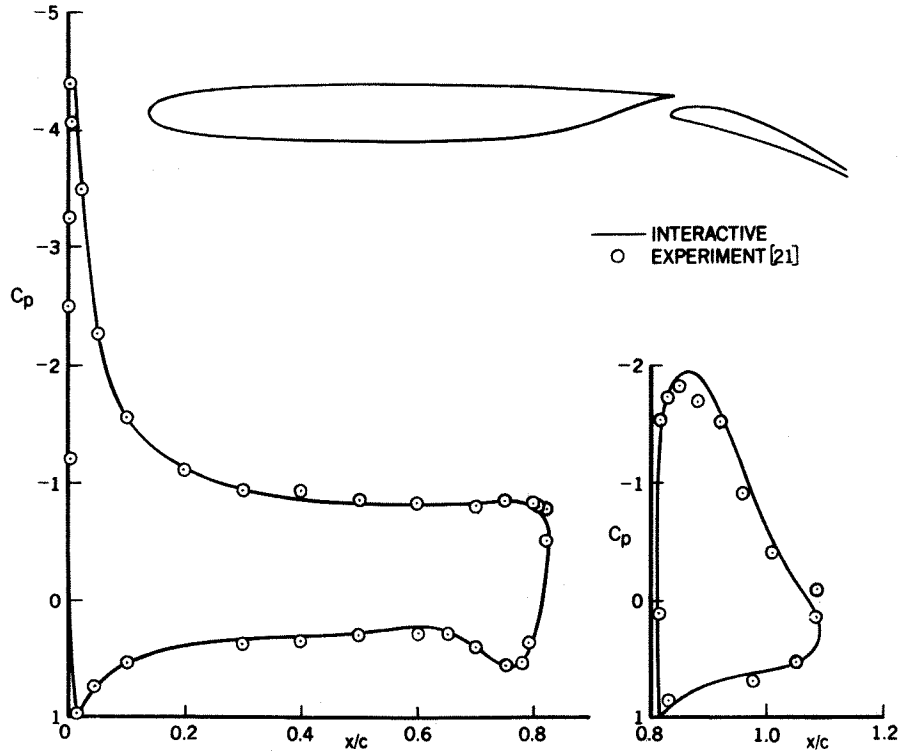

Figure 2. Comparison of calculated and measured pressure distribution for Case 2 for $\alpha = 0°$.

Figure 9 again confirms that the use of the inviscid equations leads to overprediction of lift coefficient at all angles of attack and that the interactive procedure is satisfactory up to around 8 degrees. The discrepancy at 13 degrees appears large (~7%) but is accounted for by the small differences apparent on Fig. 8 which are within experimental uncertainty, apart from those on the upper surface of the flap.

4.0 Concluding Remarks

The results of the previous section demonstrate that an interactive procedure, which can be shown to be accurate and convenient to use, can produce acceptable calculations of two-element airfoils over a range of angles of attack. The calculations were made with an algebraic eddy viscosity formulation of Cebeci and Smith[10] and without consideration of the wakes of the two elements representing an early step towards the development of a generally applicable procedure. Among the more detailed conclusions which may be drawn from the results are the following:

1. Even in its present form, the calculation method provides results which agree with experimental information within the accuracy of the

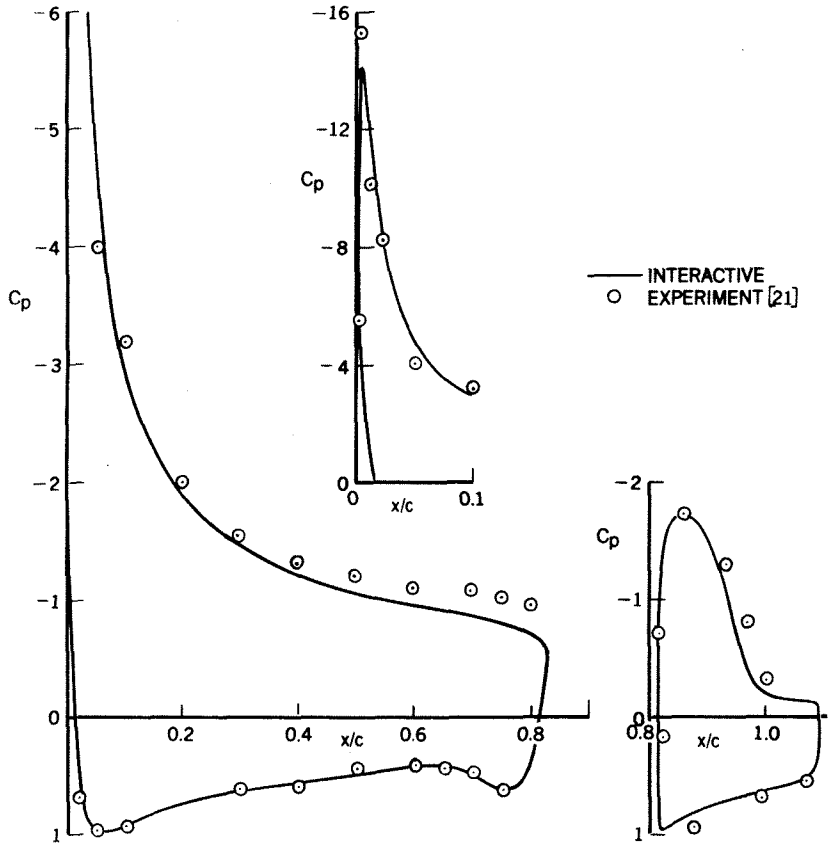

Figure 3. Comparison of calculated and measured pressure coefficients for Case 2 for $\alpha = 8.93°$.

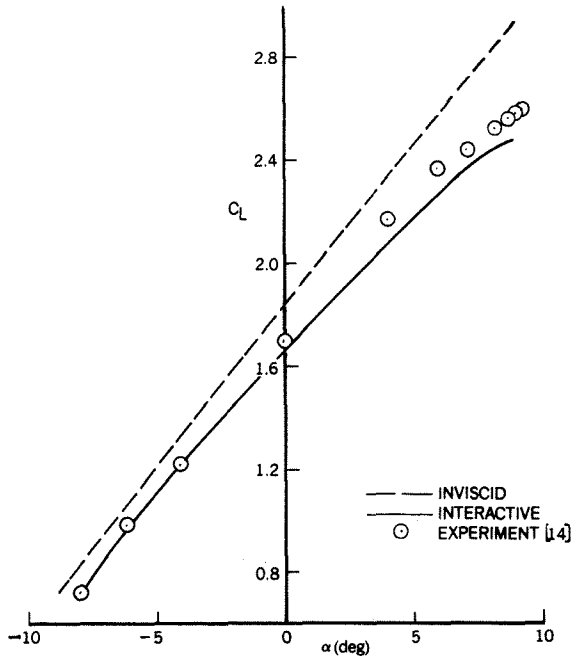

Figure 4. Comparison of calculated and measured lift coefficient, C_ℓ for Case 2.

measurements up to an angle of attack of around 10 degrees.

2. The wake of the forward element does not appear to interact with the upper-surface boundary layer in most of the cases considered, where the gaps between the elements are comparatively large, and upper-surface separation, which is readily calculated by the interactive procedure, reduces the upstream influence of the wake.

3. Small errors in the distribution of pressure coefficient around the two-element airfoils can accumulate to cause errors of up to around 8% in lift coefficient so that, in measurements or in calculations, great care is required in the interpretation of results.

In the next phase, the procedure will be extended to include the wake of both elements so that the range of accurate calculations can be extended to higher angles of attack and to configurations with small gaps between elements. The present test cases do not involve practical flap wells and the interactive procedure will also be extended to deal with them.

Acknowledgment: The research reported in this paper was sponsored by the National Science Foundation under Grant MEA 0818565.

5.0 References

1. Stevens, W.A., Goradia, S.H. and Braden, J.A.: Mathematical Model for Two-Dimensional Multi-Component Airfoils in Viscous Flow. NASA CR-1843, July 1971.

2. Van den Berg, B. and Oskam, B.: Boundary-Layer Measurements on a Two-Dimensional Wing with Flap and a Comparison with Calculations. Paper 18 of AGARD-CP-271, Sept. 1979.

3. Henderson, M.L.: Two-Dimensional Separated Wake Modeling and Its Use to Predict Maximum Section Lift Coefficient. AIAA Paper 78-156, Jan. 1978.

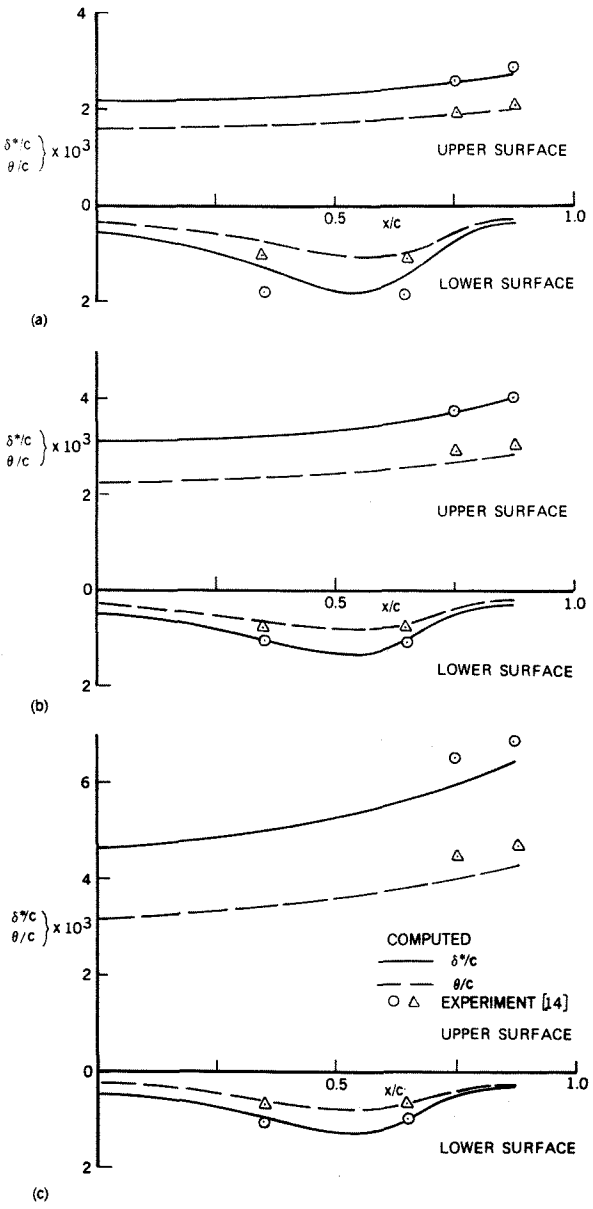

Figure 5. Comparison of calculated and measured boundary-layer parameters on the NLR 7301 wing.

4. McMasters, J.H. and Henderson, M.L.: Some Recent Applications of High-Lift Computational Methods at Boeing. J. Aircraft, Vol. 10, No. 1, Jan. 1983.

5. LeBalleur, J.C.: Couplage visqueux-non visquex: Methode Numerique et Applications Aux Ecoulements Bidimensionnels Transsoniques et Supersoniques. Le Recherche Aerospatiale No. 1978-2, 65, 1978.

6. LeBalleur, J.C.: Numerical Viscid-Inviscid Interaction in Steady and Unsteady Flows. In Numerical and Physical Aspects of Aerodynamic Flows II (ed. T. Cebeci), Springer-Verlag, NY, 259, 1984.

7. Carter, J.E.: A New Boundary-Layer Inviscid Interaction Technique for Separated Flow. AIAA Paper 79-1450, 1979.

8. Veldman, A.E.P.: New Quasi-Simultaneous Method to Calculate Interacting Boundary Layers. AIAA J. 19, 769, 1981.

9. Cebeci, T., Stewartson, K. and Williams, P.G.: Separation and Reattachment Near the Leading Edge of a Thin Airfoil at Incidence. AGARD CP 291, Paper 20, 1981.

10. Cebeci, T., Clark, R.W., Chang, K.C., Halsey, N.D. and Lee, K.: Airfoils with Separation and the Resulting Wakes. J. Fluid Mech., Vol. 153, pp. 323-347, 1986.

11. Halsey;, N.D.: Potential Flow Analysis of Multielement Airfoils Using Conformal Mapping. AIAA J., Vol. 17, p. 1281, 1979.

12. Cebeci, T.: Separated Flows and Their Representation by Boundary-Layer Equations. ONR-CR215-234-2, Mech. Eng. Rept. California State University, Long Beach, 1976.

13. Olsen, L.E. and Orloff, K.L.: On the Structure of Turbulent Wakes and Merging Shear Layers of Multi-Element Airfoils. Paper AIAA 81-1238, June 1981.

14. Omar, E., Zierten, T. and Mahal, A.: Two-Dimensional Wind Tunnel Tests of a NASA Supercritical Airfoil with Various High-Lift Systems; 1-Data Analysis. NASA CR-2214, 1973.

15. Van den Berg, B.: Boundary-Layer Measurements on a Two-Dimensional Wing with Flap. NLR TR 79009U, 1979.

16. Foster, D.N., Ashill, P.R. and Williams, B.R.: The Nature, Development and Effect of the Viscous Flow Around an Airfoil with High-Lift Devices. RAE Tech. Rept. No. 72227, 1972.

17. Halsey, N.D.: Calculaton of Compressible Potential Flow About Multielement Airfoils Using a Source Field-Panel Approach. AIAA Paper 85-0038, Jan. 1985.

18. Reyhner, J.A. and Flügge-Lotz, I.: The Interaction of a Shock Wave with a Laminar Boundary Layer. Int. J. Nonlinear Mech., Vol. 3, p. 173, 1968.

19. Bradshaw, P., Cebeci, T. and Whitelaw, J.H.: Engineering Calculation Methods for Turbulent Flows. Academic Press, 1981.

20. Cebeci, T. and Bradshaw, P.: Physical and Computational Aspects of Convective Heat Transfer. Springer-Verlag, 1985.

21. Omar, E., Zierten, T., Hahn, M., Szpiro, E. and Mahal, A.: Two-Dimensional Wind-Tunnel Tests of a NASA Supercritical Airfoil with Various High-Lift Systems; 2-Test Data. NACA Cr-2215, 1977.

22. Michel, R.: Etude de la transition sur les profiles d'aile: établissement d'un critére de determination de point de transition et calcul de la trainée de profile incompressible. ONERA Rept. 1/1578A, 1951.

23. Oskam, B., Laan, D.J. and Volkers, D.F.: Recent Advances in Computational Methods to Solve the High-Lift Multi-Component Airfoil Problem. NLR MP84042U, 1984.

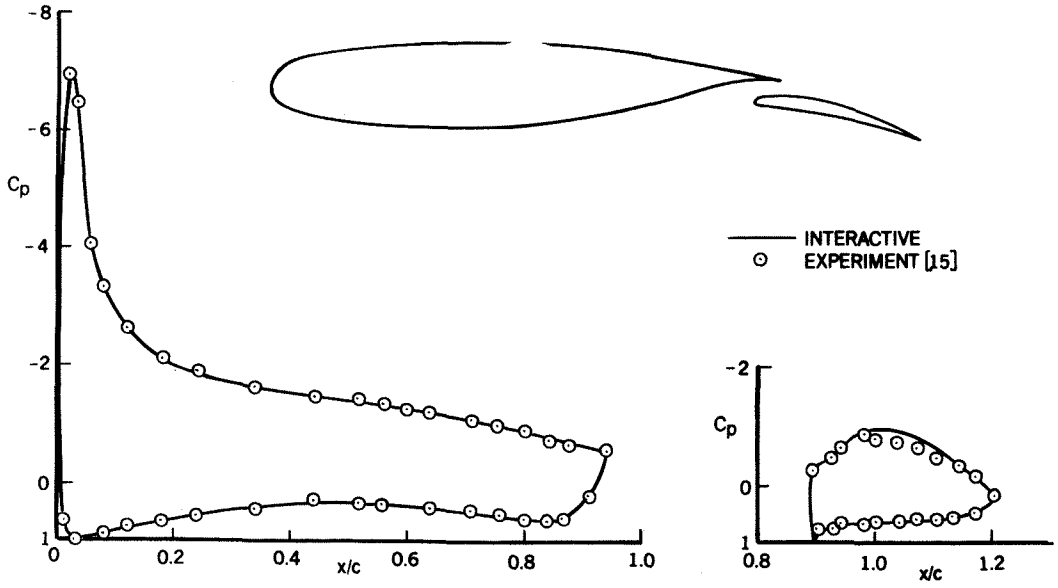

Figure 6. Comparison of calculated and measured pressure distribution on the NLR 7301 wing and flap for $\alpha = 6°$.

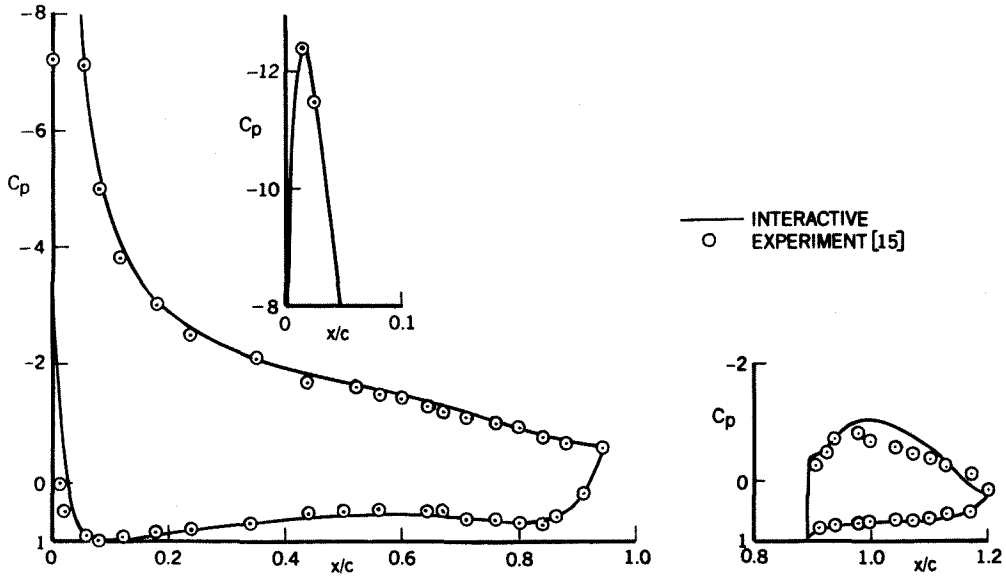

Figure 7. Comparison of calculated and measured pressure distribution on the NLR 7301 wing and flap for $\alpha = 13.1°$.

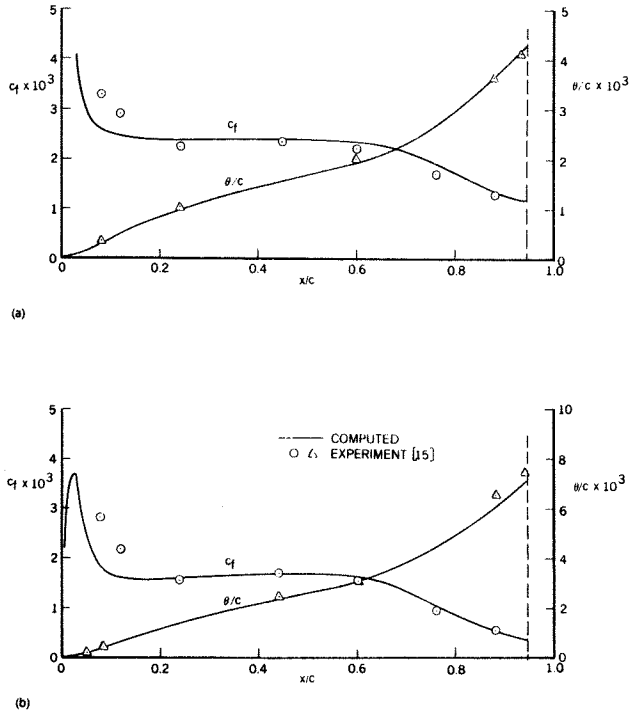

Figure 8. Comparison of calculated and measured skin-friction coefficient and momentum thickness (θ/c) on the NLR 7301 wing upper surface: (a) α = 6°, (b) α = 13.1°.

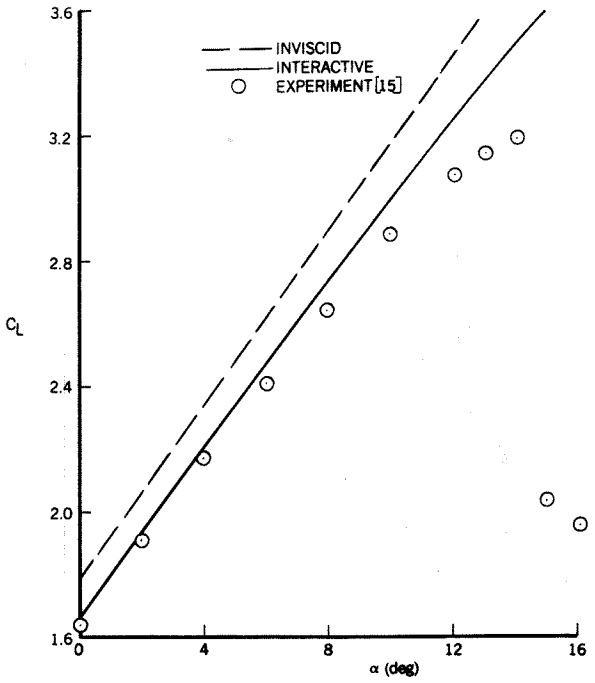

Figure 9. Comparison of calculated and measured lift coefficient of NLR 7301 wing with flap.